

An investigation of the elastic scattering of ^{17}O projectiles by different target nuclei using the CDCC method

Ş Karatepe Çelik

Hizan Vocational School, Bitlis Eren University, Bitlis, Turkey.

e-mail: skaratepe@beu.edu.tr

Received 15 March 2021; accepted 29 April 2021

The Continuum-Discretized Coupled Channels (CDCC) method is a convenient method that was developed in order to examine weakly bound nuclei. For this purpose, the elastic scattering data of ^{17}O projectile for ^{90}Zr , ^{124}Sn and ^{208}Pb target nuclei were investigated at 340 MeV using the CDCC method. In calculations using this method, ^{17}O projectiles were taken to be $^{17}\text{O} \rightarrow ^{17}\text{O} + n$. Optical potentials were selected as the interaction potentials. It was seen that the results obtained were compatible with the experimental data. The effects of excited channels in all three systems were also determined.

Keywords: Optical model; elastic scattering; CDCC Method

PACS: 24.10.Ht; 24.10.Eq

DOI: <https://doi.org/10.31349/RevMexFis.67.051202>

1. Introduction

The Continuum-Discretized Coupled Channels (CDCC) method is a quite important method for explaining the nuclear breakup processes in direct nuclear reactions involving weakly bound nuclei [1-5]. The CDCC method helps to investigate the structure of the halo nucleus as well as explaining the reaction dynamics [1,4,6]. It can be regarded as an expanded form of Coupled Channels (CC). In order to solve the CDCC method, initially, a three-body system was created. In the CDCC method, a three-body system consists of the two-body projectile and the target nucleus ($P \rightarrow C + v$). Then, a four-body system was studied by using the projectile as a three-body system. The CDCC method includes quantal bound and continuum states of the projectile. For the bound and continuum states of the projectile, the three-body Schrödinger equation solution is performed by including the three-body wave function. The continuum states were determined through the k linear and angular momentum. The k continuum is divided into thousands of parts, and this discretization is called the A_v average method [3,6-8]. The phenomenological and microscopic optical potential is generally used as the interaction potential between the projectile and the target [4].

^{17}O is the mirror nucleus of ^{17}F , and these isobars display similar features in the ground state and the first excited state. However, their neutron- and proton-binding energies are quite different from each other, such that $S_p = 0.600$ MeV for ^{17}F and $S_n = 4.143$ MeV for ^{17}O . Because these nuclei show similar properties, ^{17}O and ^{17}F nuclei were generally investigated in the same studies [9,10].

Recently, the elastic scattering of ^{17}O projectile on different targets has been studied using various methods, and many results have been obtained [9,10]. It is aimed to reproduce theoretically the experimental data and contribute to

the previous studies on the subject. Thus, this study aimed to investigate the interaction of ^{17}O projectile with different target nuclei such as ^{90}Zr , ^{124}Sn , and ^{208}Pb at 340 MeV on the Coulomb barrier, to analyze a cross-section of elastic scattering for the $^{17}\text{O} +$ target systems, and to look at the role of the excited channels. Firstly, we analyzed the elastic scattering angular distributions of $^{17}\text{O} + ^{90}\text{Zr}$, $^{17}\text{O} + ^{124}\text{Sn}$, and $^{17}\text{O} + ^{208}\text{Pb}$ systems. Then, we examined the effect of multiple channels with the CDCC method. Finally, we compared the calculated results with experimental data.

In Sec. 2, a basic description of the theoretical process is presented. Section 3 shows the results and discussion, and Sec. 4 provides the conclusion.

2. Theoretical Process

The CDCC formalism

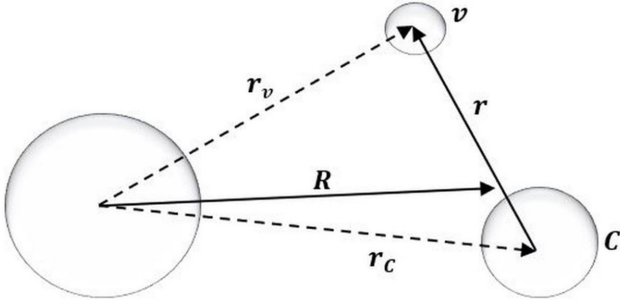
The interaction of a projectile consisting of the target (T), core (C) and a valance (v) particle that is weakly bound to it, is the equation for three-body scattering is shown below:

$$H\Psi = E\Psi. \quad (1)$$

The three-body Hamiltonian for the system is as follows:

$$H = H_{int} + T_R + U_v(r_v) + U_C(r_C). \quad (2)$$

Here, $H_{int} = T_r + v(r)$, and $v(r)$ is the interaction between the valance (v) and core (C). T_r and T_R are the kinetic energies of the projectile-target system bound by r and R . $U_C(r_C)$ and $U_v(r_v)$ are the interaction potentials of the target (T), core, and valance particle. The $T + C + v$ three-body system and Jacobi coordinates are presented in Fig. 1. The Hamiltonian is generally expressed as (r, R) in Jacobi coordinates [2,3,6].

FIGURE 1. $T + C + v$ three-body system with Jacobi coordinates.

The total wave function Ψ is determined by including the eigenfunctions of the H_{int} Hamiltonian of the projectile system. The total wave function is shown below:

$$\Psi_{CDCC} = \sum_{i=0}^N \phi_i(r) \chi_i(R). \quad (3)$$

Here, ϕ_i represents the bound and continuum states of the H_{int} Hamiltonian. $\chi_i(R)$ represents the motion between the target and the projectile. If put into the Schrödinger equation, the standard CDCC equation is represented as follows:

$$[E - T_R - \varepsilon_i] \chi_i(r) = \sum_j^N \langle \phi_i | U_j | \phi_j \rangle \chi_j(R). \quad (4)$$

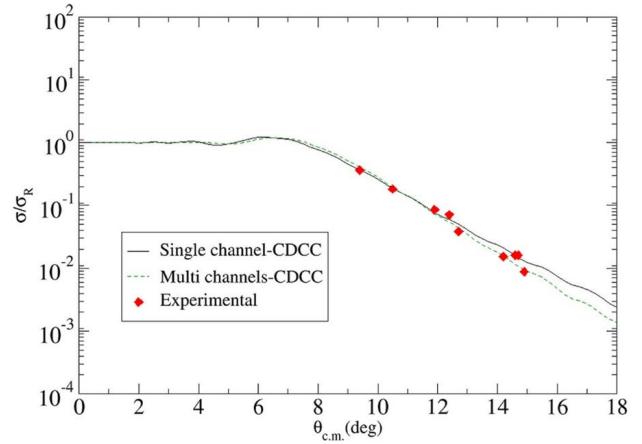
Here, $U_j = U_C(r_C) + U_v(r_v)$ and the coupling potential is

$$U_j(R) = \langle \phi_i | U_c(r_C) + U_v(r_v) | \phi_j \rangle. \quad (5)$$

In the CDCC method, continuum states for the core-valance system are represented by linear momentum (k) and angular momentum (l). The (k) continuum is divided into bins. Then, for each bin, the average of the continuum state is taken as a single state using the (Av) average method [3,11].

3. Results and discussion

Interaction between the ^{17}O projectile and the ^{90}Zr , ^{124}Sn , and ^{208}Pb target nuclei was analyzed at 340 MeV by the CDCC method. The elastic scattering cross-section results were obtained for $^{17}\text{O} + ^{90}\text{Zr}$, $^{17}\text{O} + ^{124}\text{Sn}$ and $^{17}\text{O} + ^{208}\text{Pb}$ systems. In the calculations for three interactions: core-valance, core-target, and valance-target, interaction potentials were used for a three-body system. These interaction potentials are determined as $n+^{16}\text{O}$, $^{16}\text{O}+\text{target}$ and $n+\text{target}$, respectively. $n+\text{target}$ interaction potentials were obtained by using global parameters of Koning-Delaroche and Bechetti Greenless [12,13]. Optical potential parameters for $^{16}\text{O}+\text{target}$ and $n+\text{target}$ systems are given in Tables I and II, respectively. These potentials were determined as optical potential, whose real and imaginary parts were chosen to be standard volume Woods-Saxon shapes. The calculations were performed by using the FRESCO code [14].

FIGURE 2. The elastic scattering angular distributions for the $^{17}\text{O} + ^{90}\text{Zr}$ system at 340 MeV using the CDCC method. The experimental data was taken from Ref. [15].TABLE I. Optical potential parameters for $^{16}\text{O}+\text{target}$ systems in the CDCC method

| System | V_0 (MeV) | r_0 (fm) | a_0 (fm) | W_V (MeV) | r_V (fm) | a_V (fm) |
|-----------------------------------|----------------|---------------|---------------|----------------|---------------|---------------|
| $^{16}\text{O} + ^{90}\text{Zr}$ | 100.0 | 1.1 | 0.58 | 30.0 | 1.3 | 0.7 |
| $^{16}\text{O} + ^{124}\text{Sn}$ | 55.0 | 1.2 | 0.6 | 32.0 | 1.3 | 0.7 |
| $^{16}\text{O} + ^{208}\text{Pb}$ | 60.5 | 1.07 | 0.75 | 10.0 | 1.0 | 0.8 |

TABLE II. Optical potential parameters for $n+\text{target}$ systems in the CDCC method.

| System | W_V (MeV) | r_V (fm) | a_V (fm) | W_V (MeV) | r_V (fm) | a_V (fm) |
|---------------------|----------------|---------------|---------------|----------------|---------------|---------------|
| $n+^{90}\text{Zr}$ | 54.7 | 1,21 | 0.66 | 14,6 | 1.218 | 0.66 |
| $n+^{124}\text{Sn}$ | 50.18 | 1.22 | 0.66 | 14.5 | 1.218 | 0.66 |
| $n+^{208}\text{Pb}$ | 32.68 | 1.17 | 0.75 | 5.19 | 1.32 | 0.65 |

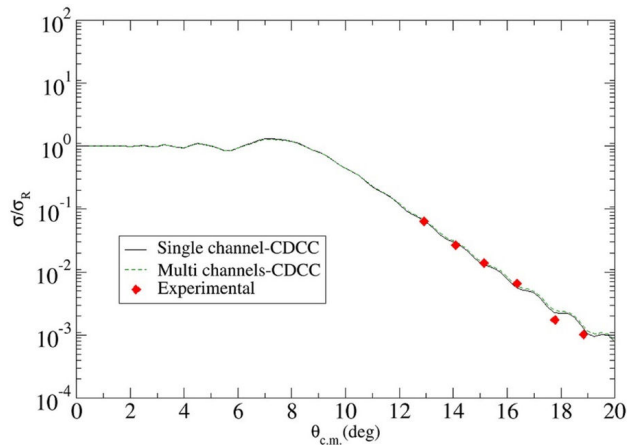


FIGURE 3. The elastic scattering angular distributions for the $^{17}\text{O} + ^{124}\text{Sn}$ system at 340 MeV using the CDCC method. The experimental data was taken from Ref. [17].

In the CDCC calculations, the continuum of the ^{17}O projectile is discretized in the k_{max} space and then divided into momentum bins with a width of Δk . The k term is the linear momentum of the $n+^{17}\text{O}$ interaction. For calculations, only $\ell \leq 3$ continuum states were taken into account.

Figure 2 shows the elastic scattering angular distribution of the $^{17}\text{O} + ^{90}\text{Zr}$ system at 340 MeV. The solid curve shows the results of single-channel CDCC calculations; the dashed curve shows the multi-channel calculations, and the red diamonds show the experimental data that was provided by Ref. [15]. It is seen that the theoretical results obtained for this reaction are quite consistent with the experimental data. The $^{16}\text{O} + ^{90}\text{Zr}$ system potential for core-target interaction was reproduced from Ref. [16]. It was seen that the breakup effect of ^{17}O is remarkable and occurs at large scattering angles; the coupling slightly increased the differential cross-sectional value. However, at small angles, there was very little effect. In this case, the effect of excited channels was considered to be small. The angular distribution for the $^{17}\text{O} + ^{124}\text{Sn}$ system at 340 MeV on the Coulomb barrier is presented in Fig. 3. Experimental data were taken from Ref. [17]. The solid curve shows the results of single-channel calculations; the dashed curve shows multichannel calculations, and the red diamonds show the experimental data. As seen in Fig. 3, the excited channel effect is rather small, and the results of CDCC calculations were quite in agreement with experimental data.

The results obtained from the $^{17}\text{O} + ^{208}\text{Pb}$ interaction at 340 MeV on the Coulomb barrier are presented in Fig. 4.

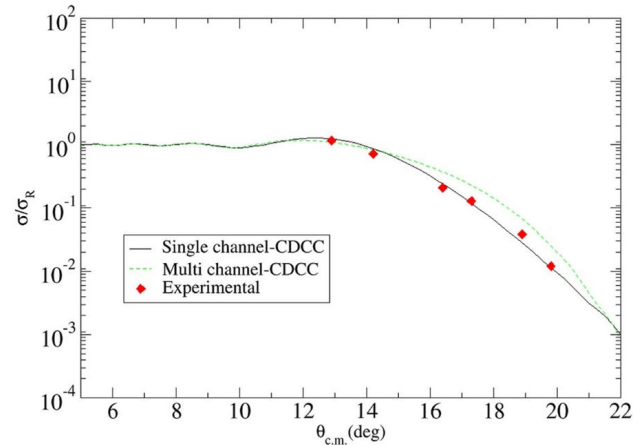


FIGURE 4. The elastic scattering angular distributions for the $^{17}\text{O} + ^{208}\text{Pb}$ system at 340 MeV using the CDCC method. The experimental data was taken from Ref. [18].

The experimental data were taken from Ref. [18]. It was seen that the results are close to the experimental data. It was also seen that the results obtained through the single-channel calculation were better than multi-channel calculation.

In this reaction, the effect of the excited channel is higher compared to the other two systems.

4. Conclusion

The CDCC method is remarkably good for investigating the reactions that involve weakly bound nuclei. In conclusion, the CDCC method was performed for three-body ^{17}O elastic scattering by three different nuclei at 340 MeV above the Coulomb barrier. The CDCC method was performed for a three-body system by taking the projectile as $^{17}\text{O} \rightarrow ^{16}\text{O}+n$, and calculations were made accordingly. The optical potential was used for the interaction potentials of the three reactions. ^{17}O -target interactions at 340 MeV displayed good agreement with experimental data. The contribution of excited channels for $^{17}\text{O} + ^{90}\text{Zr}$ and $^{17}\text{O} + ^{124}\text{Sn}$ systems was quite small. For these systems at the 340 MeV, the results show that the difference between single-channel and multi-channels is not significant. However, it was observed that excited channels affect the $^{17}\text{O} + ^{208}\text{Pb}$ system. The result is remarkable for this system at 340 MeV, and single-channel calculation explains better than multi-channel calculation the experimental data quite well. The results of these calculations show the importance of the structure of a weakly bound ^{17}O projectile nucleus.

1. I.J. Thompson, *Nucl. Phys. A* **505** (1989) 84. [https://doi.org/10.1016/0375-9474\(89\)90417-X](https://doi.org/10.1016/0375-9474(89)90417-X)
2. M. Kamimura, *Prog. of Theor. Phys. Supp.* **89** (1986) 1. <https://doi.org/10.1143/PTPS.89.1>
3. M. Yahiro *et al.*, *Prog. Theor. Exp. Phys.* (2012) 01A206.

4. K. Rusek *et al.*, *Phys. Rev. C* **72**, (2005) 037603. <https://doi.org/10.1103/PhysRevC.72.037603>
5. J. Grineviciute, P. Descouvemont, *Phys. Rev. C* **90**, (2014) 034616. <https://doi.org/10.1103/PhysRevC.90.034616>

6. A. Deltuva *et al.*, *Phys. Rev. C* **76** (2007) 064602. <https://doi.org/10.1103/PhysRevC.76.064602>
7. N. C. Summers, F. M. Nunes, I. J. Thompson, *Phys. Rev. C* **74**, (2006) 014606. <https://doi.org/10.1103/PhysRevC.74.014606>
8. T. Matsumoto *et al.*, *Phys. Rev. C* **70**, (2004) 061601(R). <https://doi.org/10.1103/PhysRevC.70.061601>
9. M. Mazzocco, *EPJ Web of Conf.* **17**, (2011) 13005. <https://doi.org/10.1051/epjconf/20111713005>
10. D. Torresi, *EPJ Web of Conf.* **117** (2016) 08027. <https://doi.org/10.1051/epjconf/201611708027>
11. M. Takashina *et al.*, *Phys. Rev. C* **67** (2003) 037601. <https://doi.org/10.1103/PhysRevC.67.037601>
12. A. J. Koning and J. P. Delaroche, *Nucl. Phys. A* **713** (2003) 231. [https://doi.org/10.1016/S0375-9474\(02\)01321-0](https://doi.org/10.1016/S0375-9474(02)01321-0)
13. F.D. Becchetti, G.W. Greenlees, *Phys. Rev.*, **182** (1969) 1190-1209. <https://doi.org/10.1103/PhysRev.182.1190>
14. I.J. Thompson, *Comput. Phys. Rep.* **7** (1988) 167.
15. F. C. L. Crespi *et al.*, *Phys. Rev. C* **91**, (2015) 024323. <https://doi.org/10.1103/PhysRevC.91.024323>
16. V. Jha *et al.*, *Eur. Phys. J. A* **15** (2002) 389. <https://doi.org/10.1140/epja/i2001-10221-1>
17. L. Pellegrini *et al.*, *Phys. Lett. B* **738** (2014) 519. <https://doi.org/10.1016/j.physletb.2014.08.029>
18. F. C. L. Crespi *et al.*, *Phys. Rev. Lett.* **113** (2014) 012501. <https://doi.org/10.1103/PhysRevLett.113.012501>